

Accepted Manuscript

Synthesis, biological evaluation, and molecular docking studies of novel 2-styryl-5-nitroimidazole derivatives containing 1,4-benzodioxan moiety as FAK inhibitors with anticancer activity

Yong-Tao Duan, Yong-Fang Yao, Wei Huang, Jigar A. Makawana, Shashikant B. Teraiya, Nilesh j. Thumar, Dan-Jie Tang, Xiang-Xiang Tao, Zhong-Chang Wang, Ai-Qin Jiang, Hai-Liang Zhu

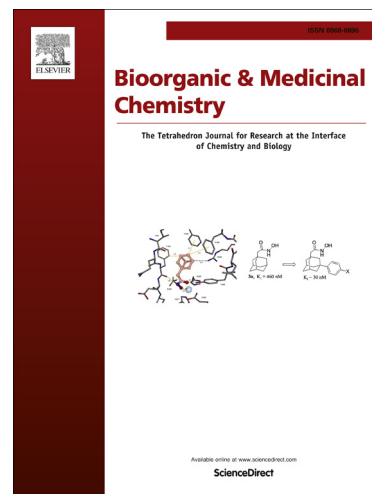
PII: S0968-0896(14)00249-1
DOI: <http://dx.doi.org/10.1016/j.bmc.2014.04.005>
Reference: BMC 11500

To appear in: *Bioorganic & Medicinal Chemistry*

Received Date: 9 March 2014
Revised Date: 2 April 2014
Accepted Date: 4 April 2014

Please cite this article as: Duan, Y-T., Yao, Y-F., Huang, W., Makawana, J.A., Teraiya, S.B., Thumar, N.j., Tang, D-J., Tao, X-X., Wang, Z-C., Jiang, A-Q., Zhu, H-L., Synthesis, biological evaluation, and molecular docking studies of novel 2-styryl-5-nitroimidazole derivatives containing 1,4-benzodioxan moiety as FAK inhibitors with anticancer activity, *Bioorganic & Medicinal Chemistry* (2014), doi: <http://dx.doi.org/10.1016/j.bmc.2014.04.005>

This is a PDF file of an unedited manuscript that has been accepted for publication. As a service to our customers we are providing this early version of the manuscript. The manuscript will undergo copyediting, typesetting, and review of the resulting proof before it is published in its final form. Please note that during the production process errors may be discovered which could affect the content, and all legal disclaimers that apply to the journal pertain.



**Synthesis, biological evaluation, and molecular docking studies of
novel 2-styryl-5-nitroimidazole derivatives
containing 1,4-benzodioxan moiety as FAK inhibitors with anticancer
activity**

**Yong-Tao Duan[†], Yong-Fang Yao[†], Wei Huang, Jigar A. Makawana, Shashikant
B. Teraiya, Nilesh j. Thumar, Dan-Jie Tang, Xiang-Xiang Tao, Zhong-Chang
Wang, Ai-Qin Jiang*, Hai-Liang Zhu***

*State Key Laboratory of Pharmaceutical Biotechnology, Medical school,
Nanjing University, Nanjing 210093, People's Republic of China*

*Corresponding author. Tel. & fax: +86-25-83592672; e-mail: zhuhl@nju.edu.cn

[†]These two authors equally contributed to this paper.

Abstract: A series of 2-styryl-5-nitroimidazole derivatives containing 1,4-benzodioxan moiety (**3a-3r**) has been designed, synthesized and their biological activities were also evaluated as potential antiproliferation and focal adhesion kinase (FAK) inhibitors. Among all the compounds, **3p** showed the most potent activity *in vitro* which inhibited the growth of A549 with IC₅₀ value of 3.11 μ M and Hela with IC₅₀ value of 2.54 μ M respectively. Compound **3p** also exhibited significant FAK inhibitory activity (IC₅₀ = 0.45 μ M). Docking simulation was performed for compound **3p** into the FAK structure active site to determine the probable binding model.

Keywords:

2-styryl-5-nitroimidazole derivatives

Focal adhesion kinase

Structure–activity relationship

Molecular docking

1.Introduction:

Focal adhesion kinase (FAK) is a 125 kDa nonreceptor tyrosine kinase that modulates cell adhesion, migration, proliferation and survival in response to extracellular signals.¹⁻⁴ In addition to being a key player in regulating normal cellular activities such as adhesion, migration and survival, FAK is also implicated in cancer cell invasion, metastasis and survival.⁵⁻⁸ Accordingly, FAK inhibition is considered as an effective antineoplastic strategy by inducing apoptosis and sensitizing tumor cells to chemotherapy. Different approaches to inhibit FAK with FAK antisense oligonucleotides,⁹⁻¹⁰ dominant-negative C-terminal domain of FAK, FAK-CD or FRNK or FAK siRNA¹¹⁻¹² caused decrease the cellular viability, growth inhibition or apoptosis. Couple of FAK inhibitors with mono- and bicyclic core structures have been reported, some of them is in clinical phase 1 testing.¹³⁻¹⁷

In previous study, metronidazole is a kind of nitroimidazole moiety has been studied extensively as radiosensitisers due to its affinity for hypoxic tumors and molecular markers of hypoxic regions in solid tumours.¹⁸ On the mechanism level, nitroimidazole derivatives have attracted considerable attention as they showed a tendency to penetrate and accumulate in regions of tumors¹⁹ and can undergo bioreduction to yield electrophilic substances which can damage protein and nucleic acids. In 2012, Dim.*et.cn* reported a series of imidazole-based candidate FAK inhibitors.²⁰ In addition, to our knowledge, few reports available in literature which described the synthesis and FAK inhibitory activity of compounds of modifications at the 2-position of the nitroimidazole ring are published. It is apparent that nitro group of metronidazole plays a key role in the metabolic activation.²¹ Metronidazole derivatives substituted in the 2-methyl group may be promising for developing new, potent and safe lead compounds.

Compounds containing 1,4-benzodioxan template also have received significant attention in chemical, medicinal and pharmaceutical research as this structural scaffold is found in a variety of drugs. For example, the mesylate salt of doxazosin is an effective drug for treatment of hypertension.²² The 6-position substituted

1,4-benzodioxan is known as a non-steroidal anti-inflammatory drug.²³ Our research group ever firstly reported that 1,4-benzodioxan moiety as potential anticancer agents targeted FAK.²⁴⁻²⁶ In continuation to extend our research on antitumor compounds with FAK inhibitory activity, herein we describe the synthesis and structure–activityrelationships of a series of 2-styryl-5-nitroimidazole derivatives containing 1,4-benzodioxan moiety as antitumor agents. Biological evaluation was also carried out for screening potential FAK inhibitors of the synthesized compounds. The apoptosis study was also carried out by flow cytometry to understand the preliminary mechanism of synthesized compounds. Docking simulations were performed to investigate the inhibitor interaction with FAK and explore the binding mode of compounds at the active site.

2. Results and discussion

2.1 Chemistry

2,3-Dihydro-benzo[1,4]dioxine-5-carboxylic acid was prepared in three steps as shown in Scheme 1. Firstly, 3,4-dihydroxybenzoic acid was catalyzed by concentrated sulfuric acid in methanol to give methyl 3,4-dihydroxybenzoate. Secondly, treatment of compound **1** with dibromoethane in acetone gave compound **2**, which was then saponified (NaOH (aq), MeOH, and THF) yielding 2,3-Dihydro-benzo[1,4]dioxine-5-carboxylic acid (compound **3**). According to method **A**, compounds **1a-1r** were synthesized by the reaction of metronidazole with different substituted benzaldehydes in DMSO by adding rapidly a stirred solution of sodium methoxide in methanol at room temperature. Synthesized compounds **1a-1r** were treated with 4-methylbenzoyl chloride using triethylamine as catalyst in CH₂Cl₂ which led to the formation of compounds **2a-2r**. The refined compounds were finally obtained by subsequent purification using chromatography. A mixture of 2,3-Dihydro-benzo[1,4]dioxine-5-carboxylic acid, compounds **2a-2r** and K₂CO₃ in DMF was refluxed to provide the desired compounds **3a-3r**. Meanwhile, the desired products could be produced following another pathway depicted in method **B**. Compound **5** was prepared according to the modified procedure of Kummerle *et al.*²⁷ Active 2,3-Dihydro-benzo[1,4]dioxine-5-carboxylic acid and metronidazole were

dissolved in CH_2Cl_2 followed by dropwise addition triethylamine giving compound **6** with yield of 85%. The target compounds **3a-3r** were synthesized by the reaction of compound **6** with different substituted benzaldehydes in DMSO by adding rapidly a stirred solution of sodium methoxide in methanol at room temperature. All synthesized compounds gave satisfactory analytical and spectroscopic data which were in full accordance with their depicted structures.

2.2. Biological activity

The inhibitory activity of the compounds is due to cell apoptosis or toxic effect, so cytotoxicity test was performed before detecting biological activity. All synthesized compounds were detected for their cytotoxicity on macrophages cells. The pharmacological results of compounds were summarized in Table 1. According to the data, it has been observed that most of the compounds were found to have low toxicity.

2.2.1 Antiproliferative activity

All the synthesized compounds **3a-3r** were screened for their *in vitro* antitumour activities against two cultured cell lines (adeno carcinomic human alveolar basal epithelial cells (A549) and human cervical cancer cell line (Hela) by CCK-8 method as compared to the potent positive control staurosporine under identical conditions. The results were mentioned in Table 1. According to Table 1, most of the synthesized compounds exhibited greater anticancer activity against one or both of the cell lines used. Among all, compounds **3p** and **3q** displayed the most potent anticancer activities (IC_{50} = 3.11, 2.54 and 5.01, 4.95 μM against A549, and Hela respectively) as comparable to positive control staurosporine with IC_{50} of 3.05, 2.72 μM against A549 and Hela).

Meanwhile, a comparison of the substitution on benzene ring was demonstrated as follows: for compounds **3a-3c**, the potency order was found as *meta*>*ortho*>*para* in -Cl substituted benzene ring while, the activity gradient was found as *para*>*meta*>*ortho* in compounds **3d-3f** containing -Br substituted benzene ring. The potent inhibitory action order could be summarized as $-\text{OCH}_3 < -\text{CH}_3 < -\text{F} < -\text{Cl} < -\text{Br}$ with change in different substitution on benzene ring. Compound **3r** with a bare phenyl

ring showed about 6-fold decreasing activity as compared to positive control. However, compound **3r** exhibited superior activity than compounds with electron-donating groups on benzene ring and inferior than compounds with electron-withdrawing groups.

From the above-mentioned analysis, it could be concluded that the compounds with electron-withdrawing groups on phenyl ring were found to be the most favorable for the antitumor activity.

2.2.2 Apoptosis analysis by Annexin V-PE fluorescence-activated cell sorting (FACS)

To test whether the inhibition of cell growth of Hela was related to cell apoptosis, Hela cell apoptosis induced by compound **3p** was determined using flow cytometry. The uptake of Annexin V-PE was significantly increased and the uptake of normal cells was significantly decreased in a time-dependent manner. Finally the percentage of early apoptotic cells was markedly elevated in a density-dependent manner from 10.60% to 4.66% at 48 h (Fig.1).

2.2.3 *Invitro* enzyme inhibition activity

To examine whether the compounds inhibit FAK, the FAK inhibitory potency of compounds **3a-3r** was examined and the results were summarized in Table 2. Most of the tested compounds displayed potent FAK inhibitory activities. Among them, compound **3p** displayed the most efficient inhibitory activity with IC_{50} value of 0.45 μ M as compared to reference drug staurosporine with IC_{50} value of 0.50 μ M. SAR analysis result of FAK inhibitory activity of the tested compounds was consistent with that of their anticancer activities. This consistency suggested that the potent anticancer activities of synthesized compounds were likely related to their FAK inhibitory activities.

2.3 Computational

2.3.1 Molecular docking

To gain better understanding on the potency of studied compounds and guide further SAR study, we proceeded to examine the interaction of compound **3p** with FAK crystal structure (2ETM pdb). The molecular docking was performed by

inserting compound **3p** into ATP binding site of FAK. All docking runs were applied CDOCKER Dock protocol of Discovery Studio 3.5. The binding modes of compound **3p** and FAK were depicted in Fig. 2. In the binding mode, compound **3p** is potently bound to the ATP binding site of FAK *via* hydrophobic interactions and binding is stabilized by two hydrogen bonds, one π -cation interaction and two charge interactions. The end group of ARG426 was formed one hydrogen bond (angle $O\cdots H-O = 124.4^\circ$, distance = 2.25 Å) with oxygen atom of 2,3-Dihydro-benzo[1,4]dioxine moiety. Meanwhile, another hydrogen bond ($O\cdots H-F = 143.3^\circ$, distance = 2.31 Å) was formed between fluorine atom and LYS454. Also the phenyl ring formed a π -cation interaction with LYS454. Besides, GLU430 and GLU506 were respectively formed two charge interactions with two nitrogen atoms. The docking calculation of all the compounds was also depicted in Table 2. The CDOCKER Energy (energy of the ligand-receptor complexes) agreed with the FAK inhibitory trend for all the synthesized compounds.

2.3.2 3D-QSAR model

In order to acquire a systematic SAR profile on 18 compounds as antitumor agents and to explore the more powerful FAK inhibitors, 3D-QSAR model was built to choose activity conformation of the designed molecular and reasonably evaluated the designed molecules by using the corresponding pIC_{50} values which were converted from the obtained IC_{50} (μM) values of FAK inhibition and performed by built-in QSAR software of DS 3.5 (Discovery Studio 3.5, Accelrys, Co. Ltd). The way of this transformation was derived from an online calculator developed from an Indian dicinal chemistry lab (<http://www.sanjeevslab.org/tools-IC50.html>). The training and test set was divided by the random diverse molecules method of DS3.5, in which the test set accounted for 83% while the training set was set to 17%. The training set composed 4 agents and 14 agents were consisted of the relative test set. The success of this model depended on docking study and the reliability of previous study about activities data.

In default situation, the alignment conformation of each molecule that possessed the lowest CDOCKER_INTERACTION_ENERGY among the ten docked poses. The

3D-QSAR model generated from DS 3.5, defined the critical regions (steric or electrostatic) affecting the binding affinity. It was a PLS model that set up 230 independent variables (conventional $R^2 = 0.84$). The graphical relationship of observed and predicted values had been illustrated in Fig. 3a, in which the plot of the observed IC_{50} versus the predicted values showed that this model could be used in prediction of activity.

A contour plot of the electrostatic field region favorable (in blue) or unfavorable (red) for anticancer activity based on telomerase target was shown in Fig. 3b while the energy grids corresponding to the favorable (in green) or unfavorable (yellow) steric effects for the telomerase affinity were shown in Fig. 3c. It was widely acceptable that a better inhibitor based on the 3D-QSAR model should have strong Van der Waals attraction in the green areas and a polar group in the blue electrostatic potential areas (which were dominant close to the skeleton). As shown in these two pictures, this promising model would provide a guideline to design and optimize more effective FAK inhibitors based on the a series of 2-styryl-5-nitroimidazole derivatives containing 1,4-benzodioxan moiety and pave the way to further study in future.

3. Conclusion

In this paper, a series of 2-styryl-5-nitroimidazole derivatives containing 1,4-benzodioxan moiety has been synthesized and evaluated for their anti-cancer activity. The bioactivity assay results showed that compound **3p** exhibited the most potent inhibitory activity for FAK with IC_{50} value of $0.45 \mu\text{M}$ as compared to the positive control staurosporine as well as good activity against A549 with IC_{50} value of $3.11 \mu\text{M}$ and Hela with IC_{50} value of $2.54 \mu\text{M}$ better than the reference drug staurosporine. The most potent inhibitor **3p** was nicely bound into active site of FAK. Also apoptosis assay results showed that compound **3p** induced apoptosis of stimulated Hela cells. Finally, QSAR models were built with previous activity data and binding conformations to provide a reliable tool for reasonable design of FAK inhibitors in the future.

4. Experiments

4.1 Chemistry

All chemicals and reagents used in the current study were of analytical grade. The reactions were monitored by thin layer chromatography (TLC) on Merck precoated silica GF254 plates. Melting points (uncorrected) were determined on a XT4 MP apparatus (Taikē Corp, Beijing, China). All the ^1H NMR spectra were recorded on a Bruker DPX 300 model Spectrometer in $\text{DMSO-}d_6$ and chemical shifts were reported in ppm (δ). Elemental analyses were performed on a CHN-O-Rapid instrument and were within $\pm 0.4\%$ of the theoretical values. ESI-MS spectra were recorded on a Mariner System 5304 Mass spectrometer.

4.2 General method of synthesis of compounds 3a-3r

Protocatechuic acid (1 mmol) in methanol (30 mL) was treated with concentrated sulfuric acid (0.5 mL) under 90°C overnight. The solvent was removed leaving oil which was dissolved in ethyl acetate (20 mL) and extracted with water (40 mL). After drying the organic layer with anhydrous Na_2SO_4 and evaporating the solvent under reduced pressure a solid appeared. The solid was recrystallized from ethanol to obtain the compound **1**. In the three-necked flask under a nitrogen atmosphere, compound **1** (1 mmol) was dissolved in dry acetone (10 mL), and then added anhydrous potassium carbonate (2 mmol). After that, the acetone solution containing dibromomethane (1 mmol) was added dropwise then refluxed for 24 h. The reaction solution was evaporated reduced pressure distillation. The appropriate amount of water was added in the residue and extracted with ethyl acetate (3×40 mL). Combined organic layer and dried with anhydrous magnesium sulfate. The solvent was removed by reduced pressure steam to give compound **2**. Compound **2** was then saponified ($\text{NaOH (aq) : MeOH : THF} = 1 : 1 : 1$) at 75°C for two hours. Filtered and recrystallization led to 2,3-Dihydro-benzo[1,4]dioxine-5-carboxylic acid (compound **3**).

Method A: Reaction of metronidazole (12 mmol) with different substituted benzaldehyde (16 mmol) in 6 mL DMSO by adding rapidly a stirred solution of sodium methoxide (12.8 mmol) in methanol at room temperature resulted in the formation of target compounds **1a-1r**. To a stirred solution of compounds **1a-1r** (7 mmol) in CH_2Cl_2 (15 mL), 4-methylbenzoyl chloride (7 mmol) and triethylamine (10

mL) at room temperature were added and stirred for 5 hours. The precipitate was purified by column chromatography using EtOAc/hexane (1:6) as eluent to give pure compounds **2a-2r**. Equimolar portions of the synthesized compounds **2a-2r** (5mmol), compound **3** (5mmol) and K₂CO₃ (5mmol) were dissolved in approximately 15 mL of DMF. The reaction solution was allowed to stir overnight at room temperature. The precipitate was purified by column chromatography using EtOAc/hexane (1:9) as eluent to give the pure compounds **3a-3r**.

Method B: SOCl₂ (10ml) was added to a stirred solution of compound **3** (20mmol) in anhydrous DMF (50 mL). The reaction solution was allowed to stir at room temperature for approximately 4 h. Then, active compound **4** (15mmol) and metronidazole (15mmol) were dissolved in CH₂Cl₂ followed by drop wise addition triethylamine and compound **5** was obtained with yield of 85%. Compound **5** (10mmol), different substituted benzaldehydes (12mmol) and NaOH (15mmol) were dissolved in DMSO (30 ml) at room temperature. The appropriate amount of water was then added in the residue and filtered. The resulting solid was collected and washed with cold water, dried and crystallized from anhydrous ethanol to get the desired compounds. All of the synthetic compounds gave satisfactory analytical and spectroscopic data, which were in full accordance with their depicted structures.

**1. (Z)-2-(2-(2-chlorostyryl)-5-nitro-1H-imidazol-1-yl)ethyl
2,3-dihydrobenzo[b][1,4]dioxine-5-carboxylate (3a)**

yield 64.5%. m.p. 188 ~ 190 °C; ¹H NMR (DMSO-*d*₆, 300 MHz) δ: 8.26 (s, 1H), 8.06 (d, *J* = 14.7 Hz, 1H), 7.99-7.79 (m, 1H), 7.54-7.47 (m, 2H), 7.43-7.35 (m, 2H), 7.09 (q, *J* = 7.9 Hz, 1H), 6.92 (q, *J* = 8.1 Hz, 1H), 6.52 (t, *J* = 7.9 Hz, 1H), 5.01 (t, *J* = 4.7 Hz, 2H), 4.58 (t, *J* = 4.7 Hz, 2H), 4.13 (s, 4H) ESI-MS: 456.09 [M+H]⁺.
Anal.Calcd for C₂₂H₁₈ClN₃O₆: C, H, N;

**2. (Z)-2-(2-(3-chlorostyryl)-5-nitro-1H-imidazol-1-yl)ethyl
2,3-dihydrobenzo[b][1,4]dioxine-5-carboxylate (3b)**

yield 64.5%. m.p. 188 ~ 189 °C; ¹H NMR (DMSO-*d*₆, 300 MHz) δ: 8.25 (s, 1H), 8.01 (t, *J* = 7.1 Hz, 2H), 7.77-7.69 (m, 2H), 7.42 (t, *J* = 7.5 Hz, 1H), 7.17 (t, *J* = 7.6

Hz, 1H), 6.93 (d, $J = 7.8$ Hz, 1H), 6.42 (d, $J = 7.9$ Hz, 2H), 5.06 (t, $J = 4.4$ Hz, 2H), 4.75 (t, $J = 4.2$ Hz, 2H), 4.17 (s, 4H), ESI-MS: 456.09 [M+H]⁺. Anal.Calcd for C₂₂H₁₈ClN₃O₆: C, H, N;

3. (Z)-2-(2-(4-chlorostyryl)-5-nitro-1H-imidazol-1-yl)ethyl

2,3-dihydrobenzo[*b*][1,4]dioxine-5-carboxylate (3c)

yield 67.5%. m.p. 187 ~ 189 °C; 1H NMR (DMSO-*d*₆, 300 MHz) δ : 8.25 (s, 1H), 7.89 (s, 1H), 7.71 (d, $J = 12.3$ Hz, 1H), 7.64-7.61 (m, 1H), 7.52 (d, $J = 7.6$ Hz, 1H), 7.42 (d, $J = 6.8$ Hz, 2H), 7.11 (d, $J = 7.9$ Hz, 1H), 6.91 (d, $J = 8.1$ Hz, 1H), 6.53-6.48 (m, 1H), 5.02 (t, $J = 8.4$ Hz, 2H), 4.57 (t, $J = 8.2$ Hz, 2H), 4.13 (s, 4H), ESI-MS: 456.09 [M+H]⁺. Anal.Calcd for C₂₂H₁₈ClN₃O₆: C, H, N;

4. (Z)-2-(2-(2-bromostyryl)-5-nitro-1H-imidazol-1-yl)ethyl

2,3-dihydrobenzo[*b*][1,4]dioxine-5-carboxylate (3d)

yield 61.5%. m.p. 188 ~ 189 °C; 1H NMR (DMSO-*d*₆, 300 MHz) δ : 8.26 (s, 1H), 7.74 (d, $J = 4.5$ Hz, 2H), 7.61 (d, $J = 6.9$ Hz, 2H), 7.47-7.32 (m, 2H), 7.13 (q, $J = 4.4$ Hz, 1H), 6.95 (q, $J = 3.3$ Hz, 1H), 6.55 (t, $J = 5.9$ Hz, 1H), 5.04 (t, $J = 4.4$ Hz, 2H), 4.59 (t, $J = 4.3$ Hz, 2H), 4.12 (s, 4H), ESI-MS: 502.04[M+H]⁺. Anal.Calcd for C₂₂H₁₈BrN₃O₆: C, H, N;

5. (Z)-2-(2-(3-bromostyryl)-5-nitro-1H-imidazol-1-yl)ethyl

2,3-dihydrobenzo[*b*][1,4]dioxine-5-carboxylate (3e)

yield 63.5%. m.p. 186 ~ 187 °C; 1H NMR (DMSO-*d*₆, 300 MHz) δ : 8.23 (s, 1H), 7.77 (d, $J = 4.4$ Hz, 2H), 7.65 (d, $J = 6.9$ Hz, 1H), 7.50-7.35 (m, 3H), 7.16 (q, $J = 4.4$ Hz, 1H), 6.99 (q, $J = 3.7$ Hz, 1H), 6.55 (t, $J = 5.9$ Hz, 1H), 5.01 (t, $J = 4.5$ Hz, 2H), 4.56 (t, $J = 4.3$ Hz, 2H), 4.13 (s, 4H), ESI-MS: 502.04[M+H]⁺. Anal.Calcd for C₂₂H₁₈BrN₃O₆: C, H, N;

6. (Z)-2-(2-(4-bromostyryl)-5-nitro-1H-imidazol-1-yl)ethyl

2,3-dihydrobenzo[*b*][1,4]dioxine-5-carboxylate (3f)

yield 62.5%. m.p. 187 ~ 189 °C; ¹H NMR (DMSO-*d*₆, 300 MHz) δ: 8.25 (s, 1H), 7.74-7.67 (m, 3H), 7.60 (d, *J* = 9 Hz, 2H), 7.47 (d, *J* = 14.6 Hz, 1H), 7.10 (q, *J* = 4.0 Hz, 1H), 6.92 (q, *J* = 3.6 Hz, 1H), 6.52 (t, *J* = 7.9 Hz, 1H), 4.99 (t, *J* = 4.4 Hz, 2H), 4.56 (t, *J* = 4.5 Hz, 2H), 4.13 (s, 4H), ESI-MS: 502.04[M+H]⁺. Anal.Calcd for C₂₂H₁₈BrN₃O₆: C, H, N;

7. (Z)-2-(2-(2-fluorostyryl)-5-nitro-1*H*-imidazol-1-yl)ethyl 2,3-dihydrobenzo[*b*][1,4]dioxine-5-carboxylate (3g)

yield 64.5%. m.p. 188 ~ 189 °C; ¹H NMR (DMSO-*d*₆, 300 MHz) δ: 8.25 (s, 1H), 7.92 (t, *J* = 7.9 Hz, 1H), 7.83 (d, *J* = 6.9 Hz, 1H), 7.51-7.40 (m, 2H), 7.29-7.23 (m, 2H), 7.10 (q, *J* = 3.9 Hz, 1H), 6.90 (q, *J* = 4.0 Hz, 1H), 6.50 (t, *J* = 7.9 Hz, 1H), 4.99 (t, *J* = 4.7 Hz, 2H), 4.58 (t, *J* = 4.7 Hz, 2H), 4.13 (s, 4H), ESI-MS: 440.12[M+H]⁺. Anal.Calcd for C₂₂H₁₈FN₃O₆: C, H, N;

8. (Z)-2-(2-(3-fluorostyryl)-5-nitro-1*H*-imidazol-1-yl)ethyl 2,3-dihydrobenzo[*b*][1,4]dioxine-5-carboxylate (3h)

yield 62.5%. m.p. 188 ~ 189 °C; ¹H NMR (DMSO-*d*₆, 300 MHz) δ: 8.23 (s, 1H), 7.97 (d, *J* = 6.9 Hz, 1H), 7.86 (d, *J* = 6.9 Hz, 1H), 7.55-7.44 (m, 3H), 7.29 (d, *J* = 4.5 Hz, 1H), 7.14 (q, *J* = 3.3 Hz, 1H), 6.94 (q, *J* = 4.4 Hz, 1H), 6.56 (t, *J* = 7.9 Hz, 1H), 4.95 (t, *J* = 4.4 Hz, 2H), 4.55 (t, *J* = 4.3 Hz, 2H), 4.13 (s, 4H), ESI-MS: 440.12[M+H]⁺. Anal.Calcd for C₂₂H₁₈FN₃O₆: C, H, N;

9. (Z)-2-(2-(4-fluorostyryl)-5-nitro-1*H*-imidazol-1-yl)ethyl 2,3-dihydrobenzo[*b*][1,4]dioxine-5-carboxylate (3i)

yield 65.5%. m.p. 188 ~ 190 °C; ¹H NMR (DMSO-*d*₆, 300 MHz) δ: 8.21 (s, 1H), 7.95 (t, *J* = 6.9 Hz, 1H), 7.85 (d, *J* = 6.9 Hz, 2H), 7.51 (d, *J* = 6.6 Hz, 2H), 7.29 (m, 1H), 7.14 (q, *J* = 3.3 Hz, 1H), 6.96 (q, *J* = 4.4 Hz, 1H), 6.54 (t, *J* = 7.7 Hz, 1H), 4.96 (t, *J* = 4.4 Hz, 2H), 4.58 (t, *J* = 4.4 Hz, 2H), 4.11 (s, 4H), ESI-MS: 440.12[M+H]⁺. Anal.Calcd for C₂₂H₁₈FN₃O₆: C, H, N;

**10. (Z)-2-(2-(2-methylstyryl)-5-nitro-1H-imidazol-1-yl)ethyl
2,3-dihydrobenzo[*b*][1,4]dioxine-5-carboxylate (3j)**

yield 66.5%. m.p. 187~ 188 °C; ¹H NMR (DMSO-*d*₆, 300 MHz) δ: 8.26 (s, 1H), 7.93 (t, *J* = 6.6 Hz, 1H), 7.83 (t, *J* = 6.6 Hz, 2H), 7.58 (d, *J* = 3.6 Hz, 1H), 7.33 (m, 2H), 7.16 (q, *J* = 3.6 Hz, 1H), 6.99 (q, *J* = 4.8 Hz, 1H), 6.57(t, *J* = 7.8 Hz, 1H), 4.95 (t, *J* = 4.4 Hz, 2H), 4.62 (t, *J* = 4.8 Hz, 2H), 4.12 (s, 4H), 2.32 (s, 3H), ESI-MS: 436.14[M+H]⁺. Anal.Calcd for C₂₃H₂₁N₃O₆: C, H, N;

**11. (Z)-2-(2-(3-methylstyryl)-5-nitro-1H-imidazol-1-yl)ethyl
2,3-dihydrobenzo[*b*][1,4]dioxine-5-carboxylate (3k)**

yield 62.5%. m.p. 188 ~ 190 °C; ¹H NMR (DMSO-*d*₆, 300 MHz) δ: 8.24 (s, 1H), 7.90 (d, *J* = 6.9 Hz, 1H), 7.82 (t, *J* = 6.6 Hz, 2H), 7.56 (d, *J* = 3.6 Hz, 1H), 7.29 (m, 2H), 7.18 (q, *J* = 3.6 Hz, 1H), 6.94 (q, *J* = 4.4 Hz, 1H), 6.62 (t, *J* = 7.3 Hz, 1H), 4.98 (t, *J* = 4.8 Hz, 2H), 4.61 (t, *J* = 4.8 Hz, 2H), 4.13 (s, 4H), 2.25 (s, 3H), ESI-MS: 436.14[M+H]⁺. Anal.Calcd for C₂₃H₂₁N₃O₆: C, H, N;

**12. (Z)-2-(2-(4-methylstyryl)-5-nitro-1H-imidazol-1-yl)ethyl
2,3-dihydrobenzo[*b*][1,4]dioxine-5-carboxylate (3l)**

yield 68.5%. m.p. 189 ~ 190 °C; ¹H NMR (DMSO-*d*₆, 300 MHz) δ: 8.27 (s, 1H), 7.85 (d, *J* = 12.9 Hz, 1H), 7.46-7.39 (m, 3H), 7.36-7.26 (m, 2H), 7.07 (q, *J* = 3.8 Hz, 1H), 6.90 (q, *J* = 3.3 Hz, 1H), 6.57 (t, *J* = 7.9 Hz, 1H), 4.87 (t, *J* = 7.7 Hz, 2H), 4.58 (t, *J* = 4.6 Hz, 2H), 4.13 (s, 4H), 2.43 (s, 3H) ESI-MS: 436.14[M+H]⁺. Anal.Calcd for C₂₃H₂₁N₃O₆: C, H, N;

**13. (Z)-2-(2-(2-methoxystyryl)-5-nitro-1H-imidazol-1-yl)ethyl
2,3-dihydrobenzo[*b*][1,4]dioxine-5-carboxylate (3m)**

yield 66.5%. m.p. 188 ~ 190 °C; ¹H NMR (DMSO-*d*₆, 300 MHz) δ: 8.21 (s, 1H), 7.81 (d, *J* = 4.5 Hz, 1H), 7.41 (t, *J* = 6.3 Hz, 1H), 7.44-7.28 (m, 4H), 6.98 (t, *J* = 5.1 Hz, 2H), 6.52 (t, *J* = 5.8 Hz, 1H), 4.96 (t, *J* = 3.3, 2H), 4.62 (t, *J* = 6.5 Hz, 2H), 4.16 (s, 4H), 3.76 (s, 3H), ESI-MS: 452.14 [M+H]⁺. Anal.Calcd for C₂₃H₂₁N₃O₇: C, H, N;

**14. (Z)-2-(2-(3-methoxystyryl)-5-nitro-1H-imidazol-1-yl)ethyl
2,3-dihydrobenzo[b][1,4]dioxine-5-carboxylate (3n)**

yield 68.5%. m.p. 187 ~ 188 °C; ¹H NMR (DMSO-*d*₆, 300 MHz) δ: 8.23 (s, 1H), 7.71 (d, *J* = 14.5 Hz, 1H), 7.41 (d, *J* = 14.3 Hz, 1H), 7.34-7.25 (m, 3H), 7.10 (d, *J* = 7.8 Hz, 1H), 6.92 (t, *J* = 9.1 Hz, 2H), 6.49 (t, *J* = 7.8 Hz, 1H), 4.99 (t, *J* = 4.3 Hz, 2H), 4.55 (t, *J* = 4.5 Hz, 2H), 4.11 (s, 4H), 3.77 (s, 3H), ESI-MS: 452.14 [M+H]⁺. Anal.Calcd for C₂₃H₂₁N₃O₇: C, H, N;

**15. (Z)-2-(2-(4-methoxystyryl)-5-nitro-1H-imidazol-1-yl)ethyl
2,3-dihydrobenzo[b][1,4]dioxine-5-carboxylate (3o)**

yield 65.5%. m.p. 188 ~ 189 °C; ¹H NMR (DMSO-*d*₆, 300 MHz) δ: 8.18 (s, 1H), 7.79 (d, *J* = 6.5 Hz, 2H), 7.44-7.31 (m, 3H), 7.21 (d, *J* = 4.8 Hz, 2H), 6.98 (t, *J* = 6.1 Hz, 2H), 6.51 (t, *J* = 7.8 Hz, 2H), 4.97 (t, *J* = 4.4 Hz, 2H), 4.57 (t, *J* = 4.5 Hz, 2H), 4.14 (s, 4H), 3.75 (s, 3H), ESI-MS: 452.14 [M+H]⁺. Anal.Calcd for C₂₃H₂₁N₃O₇: C, H, N;

**16. (Z)-2-(2-(2-chloro-6-fluorostyryl)-5-nitro-1H-imidazol-1-yl)ethyl
2,3-dihydrobenzo[b][1,4]dioxine-5-carboxylate (3p)**

yield 67.5%. m.p. 187 ~ 189 °C; ¹H NMR (DMSO-*d*₆, 300 MHz) δ: 8.27 (s, 1H), 7.85 (d, *J* = 12.5 Hz, 1H), 7.43-7.26 (m, 4H), 7.08-7.05 (m, 1H), 6.92-6.88 (m, 1H), 6.60-6.54 (m, 1H), 4.87 (t, *J* = 4.6 Hz, 2H), 4.58 (t, *J* = 4.6 Hz, 2H), 4.12 (s, 4H), ESI-MS: 474.08 [M+H]⁺. Anal.Calcd for C₂₂H₁₇FCIN₃O₆: C, H, N;

**17. (Z)-2-(2-(2-(naphthalen-1-yl)vinyl)-5-nitro-1H-imidazol-1-yl)ethyl
2,3-dihydrobenzo[b][1,4]dioxine-5-carboxylate (3q)**

yield 68.5%. m.p. 187 ~ 189 °C; ¹H NMR (DMSO-*d*₆, 300 MHz) δ: 8.26 (s, 1H), 7.85 (d, *J* = 5.8 Hz, 1H), 7.55-7.32 (m, 4H), 7.18-7.08 (m, 4H), 6.82 (t, *J* = 4.8 Hz, 2H), 6.65 (d, *J* = 3.9 Hz, 1H), 4.86 (t, *J* = 4.7 Hz, 2H), 4.57 (t, *J* = 4.6 Hz, 2H), 4.13 (s, 4H), ESI-MS: 472.14 [M+H]⁺. Anal.Calcd for C₂₆H₂₁N₃O₆: C, H, N;

**18. (Z)-2-(5-nitro-2-styryl-1H-imidazol-1-yl)ethyl
2,3-dihydrobenzo[b][1,4]dioxine-5-carboxylate (3r)**

yield 66.5%. m.p. 188 ~ 189 °C; ¹H NMR (DMSO-*d*₆, 300 MHz) δ : 8.25 (s, 1H), 7.88 (d, *J* = 5.5 Hz, 1H), 7.45-7.25 (m, 4H), 7.08-7.05 (m, 3H), 6.92 (d, *J* = 4.4 Hz, 1H), 6.60 (d, *J* = 3.3 Hz, 1H), 4.89 (t, *J* = 4.4 Hz, 2H), 4.55 (t, *J* = 4.6 Hz, 2H), 4.13 (s, 4H), ESI-MS: 422.13 [M+H]⁺. Anal. Calcd for C₂₂H₁₈N₃O₆: C, H, N;

5. Bioassay conditions

5.1 FAK inhibitory assay

To evaluate the effect of the compounds on FAK assembly *in vitro*, varying concentrations were pre-incubated with 10 μ MFAK in glutamate buffer at 30 °C and then cooled to 0°C. After addition of GTP, the mixtures were transferred to 0°C cuvettes in a recording spectrophotometer and warmed up to 30 °C and the assembly of FAK was observed turbid metrically. The IC₅₀ was defined as the compound concentration that inhibited the extent of assembly by 50% after 20 min incubation.

5.2 Cell proliferation assay

CCK-8 is much more convenient and helpful than MTT for analyzing cell proliferation, because it can be reduced to soluble formazan by dehydrogenase in mitochondria and has little toxicity to cells. Cell proliferation was determined using CCK-8 dye (BeyotimeInst Biotech, China) according to manufacture's instructions. Briefly, 1-5 $\times 10^3$ cells per well were seeded in a 96-well plate, grown at 37 °C for 12 h. Subsequently, cells were treated with the target compounds at increasing concentrations in the presence of 10% FBS for 24 or 48 h. After 10 μ L CCK-8 dye was added to each well, cells were incubated at 37 °C for 1-2 h and Plates were read in a Victor-V multilabel counter (Perkin-Elmer) using the default europium detection protocol. Percent inhibition or IC₅₀ values of compounds were calculated by comparison with DMSO-treated control wells.

5.3 Flow cytometry

Cells (1.3 $\times 10^5$ cells/mL) were cultured in the presence or not of novobiocin analogues at 200 μ M. Nvb at the same concentration served as reference inhibitor.

After treatment for 48 and 72 h, cells were washed and fixed in PBS/ ethanol (30/70). For cytofluorometric examination, cells (10^4 cells/mL) were incubated for 30 min in PBS/ Triton X100, 0.2% /EDTA 1 mM, and propidium iodide (PI) ($50 \mu\text{g/mL}$) in PBS supplemented by RNase (0.5 mg/mL). The number of cells in the different phases of the cell cycle was determined, and the percentage of apoptotic cells was quantified. Analyses were performed with a FACS Calibur (Becton Dickinson, Le Pont de Claix, France). Cell Quest software was used for data acquisition and analysis.

6. Virtual calculation

6.1 Experimental protocol of docking study

Molecular docking of compounds **3a-3r** into the FAK catalytic subunit (PDB code: 2ETM) was carried out using the Auto-Dock software package (version 3.5) as implemented through the graphical user interface Auto-DockTools (ADT 1.4.6).

6.2 3D-QSAR

Ligand-based 3D-QSAR approach was performed by QSAR software of DS 3.5 (Discovery Studio 3.5, Accelrys, Co.Ltd). The training sets were composed of inhibitors with the corresponding pIC_{50} values which were converted from the obtained IC_{50} (μM), and test sets comprised compounds of data sets. All the definition of the descriptors can be seen in the “Help” of DS 3.5 software and they were calculated by QSAR protocol of DS 3.5. The alignment conformation of each molecule was the one with lowest interaction energy in the docked results of CDOCKER. The predictive ability of 3D-QSAR modeling can be evaluated based on the cross-validated correlation coefficient, which qualifies the predictive ability of the models. Scrambled test (Y scrambling) was performed to investigate the risk of chance correlations. The inhibitory potencies of compounds were randomly reordered for 30 times and subject to leave-one-out validation test, respectively. The models were also validated by test sets, in which the compounds are not included in the training sets. Usually, one can believe that the modeling is reliable, when the R^2 for test sets is larger than 0.6.

Acknowledgment

This work was supported by the project (No. **BY2012136**) from the Science &

Technology Agency of Jiangsu Province and by the projects (Nos.CXY1213&CXY1222) from the Science & Technology Bureau of Lianyungang City of Jiangsu Province.

Reference

1. Hall, J. E.; Fu, W.; Schaller, M. D. *Int Rev Cell Mol Biol***2011**, *288*, 185.
2. Hochwald, S. N.; Golubovskaya, G. *Gene Ther Mol Biol***2009**, *13*, 26.
3. Peng, X.; Guan, J.-L. *Current Protein and Peptide Science***2011**, *12*, 52.
4. Schlaepfer, D. D.; Mitra, S. K. *Current opinion in genetics & development***2004**, *14*, 92.
5. Cance, W. G.; Harris, J. E.; Iacocca, M. V.; Roche, E.; Yang, X.; Chang, J.; Simkins, S.; Xu, L. *Clinical Cancer Research***2000**, *6*, 2417.
6. Hao, H.; Naomoto, Y.; Bao, X.; Watanabe, N.; Sakurama, K.; Noma, K.; Motoki, T.; Tomono, Y.; Fukazawa, T.; Shirakawa, Y. *Oncology reports***2009**, *22*, 973.
7. Yang, X.-H.; Xiang, L.; Li, X.; Zhao, T.-T.; Zhang, H.; Zhou, W.-P.; Wang, X.-M.; Gong, H.-B.; Zhu, H.-L. *Bioorganic & medicinal chemistry***2012**, *20*, 2789.
8. Zhang, S.; Luo, Y.; He, L.-Q.; Liu, Z.-J.; Zhu, H.-L. *Bioorganic & medicinal chemistry***2013**.
9. Ballabeni, V.; Banerjee, D.; Banik, I.; Baoshan, W.; Bapna, S.; Ardisson, J.; Aubert, G.; Awad, H.; Ayoub, M.; Azas, N. *European Journal of Medicinal Chemistry***2010**, *45*, 6221.
10. Smith, C. S.; Golubovskaya, V. M.; Peck, E.; Xu, L.-H.; Monia, B. P.; Yang, X.; Cance, W. G. *Melanoma research***2005**, *15*, 357.
11. Demirbas, A.; Sahin, D.; Demirbas, N.; Karaoglu, S. A. *European journal of medicinal chemistry***2009**, *44*, 2896.
12. Halder, J.; Landen, C. N.; Lutgendorf, S. K.; Li, Y.; Jennings, N. B.; Fan, D.; Nelkin, G. M.; Schmandt, R.; Schaller, M. D.; Sood, A. K. *Clinical cancer research***2005**, *11*, 8829.
13. de Courcy, B.; Piquemal, J.-P.; Garbay, C.; Gresh, N. *Journal of the American Chemical Society***2010**, *132*, 3312.
14. Halder, J.; Lin, Y. G.; Merritt, W. M.; Spannuth, W. A.; Nick, A. M.; Honda, T.;

- Kamat, A. A.; Han, L. Y.; Kim, T. J.; Lu, C. *Cancer research***2007**, *67*, 10976.
15. Hochwald, S. N.; Nyberg, C.; Zheng, M.; Zheng, D.; Wood, C.; Massoll, N. A.; Magis, A.; Ostrov, D. A.; Cance, W. G.; Golubovskaya, V. M. *Cell cycle***2009**, *8*, 2435.
16. Infante, J. R.; Camidge, D. R.; Mileskin, L. R.; Chen, E. X.; Hicks, R. J.; Rischin, D.; Fingert, H.; Pierce, K. J.; Xu, H.; Roberts, W. G. *Journal of Clinical Oncology***2012**, *30*, 1527.
17. Zheng, D.; Golubovskaya, V.; Kurenova, E.; Wood, C.; Massoll, N. A.; Ostrov, D.; Cance, W. G.; Hochwald, S. N. *Molecular carcinogenesis***2010**, *49*, 200.
18. Giglio, J.; Fernández, S.; Rey, A.; Cerecetto, H. *Bioorganic & medicinal chemistry letters***2011**, *21*, 394.
19. Born, J. L.; Smith, B. R.; Harper, N.; Koch, C. J. *Biochemical pharmacology***1992**, *43*, 1337.
20. Dimova, D.; Iyer, P.; Vogt, M.; Totzke, F.; Kubbutat, M. H.; Schächtele, C.; Laufer, S.; Bajorath, J. *Journal of medicinal chemistry***2012**, *55*, 11067.
21. Shimamura, M.; Nagasawa, H.; Ashino, H.; Yamamoto, Y.; Hazato, T.; Uto, Y.; Hori, H.; Inayama, S. *British journal of cancer***2003**, *88*, 307.
22. Altiokka, G.; Atkosar, Z.; Can, N. *Journal of pharmaceutical and biomedical analysis***2002**, *30*, 881.
23. Quaglia, W.; Santoni, G.; Pigni, M.; Piergentili, A.; Gentili, F.; Buccioni, M.; Mosca, M.; Lucciarini, R.; Amantini, C.; Nabissi, M. I. *Journal of medicinal chemistry***2005**, *48*, 7750.
24. Hou, Y.-P.; Sun, J.; Pang, Z.-H.; Lv, P.-C.; Li, D.-D.; Yan, L.; Zhang, H.-J.; Zheng, E. X.; Zhao, J.; Zhu, H.-L. *Bioorganic & medicinal chemistry***2011**, *19*, 5948.
25. Sun, J.; Yang, Y.-S.; Li, W.; Zhang, Y.-B.; Wang, X.-L.; Tang, J.-F.; Zhu, H.-L. *Bioorganic & medicinal chemistry letters***2011**, *21*, 6116.
26. Zhang, X.-M.; Qiu, M.; Sun, J.; Zhang, Y.-B.; Yang, Y.-S.; Wang, X.-L.; Tang, J.-F.; Zhu, H.-L. *Bioorganic & medicinal chemistry***2011**, *19*, 6518.
27. Kümmerle, A. E.; Schmitt, M.; Cardozo, S. V.; Lugnier, C.; Villa, P.; Lopes, A. B.; Romeiro, N. C.; Justiniano, H. I. n.; Martins, M. A.; Fraga, C. A. *Journal of Medicinal Chemistry***2012**, *55*, 7525.

Legends

Figure 1.Compound **3p** induced apoptosis in HELA cells with the density of 1.6, 8.0, 40.0, 200.0 $\mu\text{g/mL}$. HELA cells were treated with for 48 h.

Figure 2.Molecular docking modeling of compound **3p** with tubulin: **(2A)** 2D Ligand interaction diagram of compound **3p** with PLK1. **(2B)** 3D model of the interaction between compound **3p** and the PLK1 binding site.

Figure 3.**(3A)** Using linear fitting curve to compare the predicted pIC_{50} value with that of experiment.**(3B)** Isosurface of the 3D-QSAR model coefficients on electrostatic potential grids. The blue triangle mesh represents positive electrostatic potential and the red area represents negative electrostatic potential. **(3C)** Isosurface of the 3D-QSAR model coefficients on Van der Waals grids. The green triangle mesh representation indicates positive coefficients; the yellow triangle mesh indicates negative coefficients.

Scheme 1.General method of the preparation of compounds **3a-3r**. Reagents and conditions: (I) methanol, concentrated sulfuric acid, 90°C , 8 h; (II) dibromoethane, potassium carbonate, acetone, 70°C , 12 h; (III) NaOH (aq), MeOH, THF (85–95%); Method **A**: (IV) Sodium methoxide, different aldehydes, DMSO, methanol, room temperature, 4h; (V) 4-toluene sulfonyl chloride; CH_2Cl_2 , TEA, room temperature, 5 h. (VI) 2,3-dihydro-1,4-benzodioxine-5-carboxylic acid, DMF, K_2CO_3 , reflux, overnight; Method **B**: (VII) SOCl_2 , DMF, reflux, 4 h; (VIII) CH_2Cl_2 , TEA, 8 h. (IX) NaOH, different aldehydes, DMSO, methanol, room temperature, overnight.

Table 1

In vitro anticancer activities (IC₅₀, μ M) of compounds **3a** – **3r** against human tumor cell lines and cytotoxicity assay of the compounds on macrophages cells (CC₅₀, μ M).

Compounds	CC ₅₀	IC ₅₀	
		A549	Hela
3a	20.32	10.54	8.97
3b	18.34	7.87	5.90
3c	12.27	15.76	12.78
3d	13.32	14.33	12.54
3e	14.43	12.34	11.71
3f	20.40	7.54	9.76
3g	19.23	8.21	7.10
3h	15.44	9.09	9.90
3i	17.89	10.55	15.23
3j	10.43	17.23	21.44
3k	6.45	15.73	16.25
3l	7.67	18.66	12.48
3m	15.65	21.78	17.67
3n	8.43	17.65	21.56
3o	6.67	20.55	25.23
3p	35.53	3.11	2.54
3q	26.55	5.01	4.95
3r	11.43	16.23	15.01
Staurosporine	-	3.05	2.72

Table 2Fak inhibitory activity and docking calculation of compounds **3a-3r**.

Compounds	IC ₅₀ (μ M)	Δ Gb (-kcal/mol)	Compounds	IC ₅₀ (μ M)	Δ Gb (-kcal/mol)
	Tubulininhibition	CDocker Energy		Tubulininhibition	CDocker Energy
3a	6.55	51.43	3k	16.21	43.21
3b	3.42	58.34	3l	26.54	31.45
3c	18.42	40.65	3m	30.07	29.56
3d	12.43	46.11	3n	24.43	33.43
3e	10.34	48.23	3o	28.67	29.78
3f	1.75	60.31	3p	0.45	68.71
3g	4.34	55.34	3q	1.01	64.11
3h	5.21	52.78	3r	20.56	38.65
3i	8.01	50.02	Staurosporine ^a	0.50	-
3j	23.54	35.32			

^aUsed as a positive control

Figure 1. Compound **3p** induced apoptosis in HELA cells with the density of 1.6, 8.0, 40.0, 200.0 $\mu\text{g/mL}$. HELA cells were treated with for 48 h.

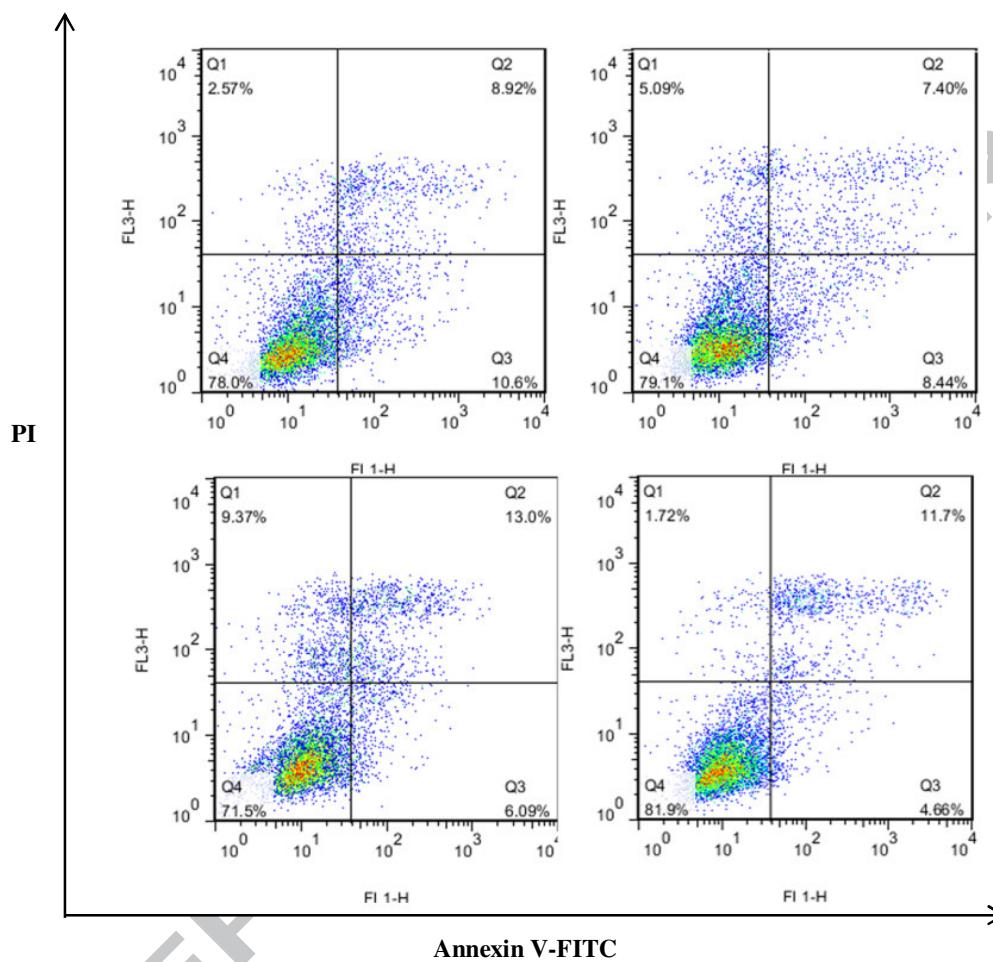
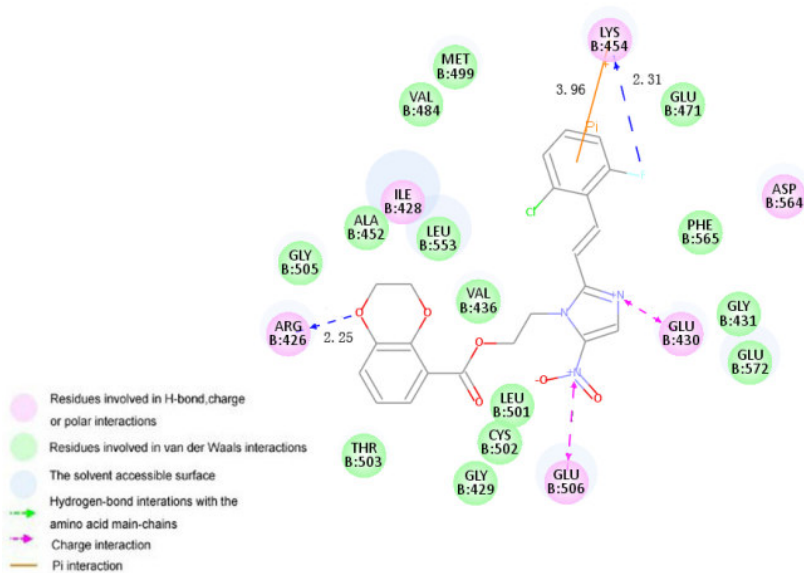


Figure 2. Molecular docking modeling of compound **3p** with tubulin: **(2A)** 2D Ligand interaction diagram of compound **3p** with PLK1. **(2B)** 3D model of the interaction between compound **3p** and the PLK1 binding site.

2A



2B

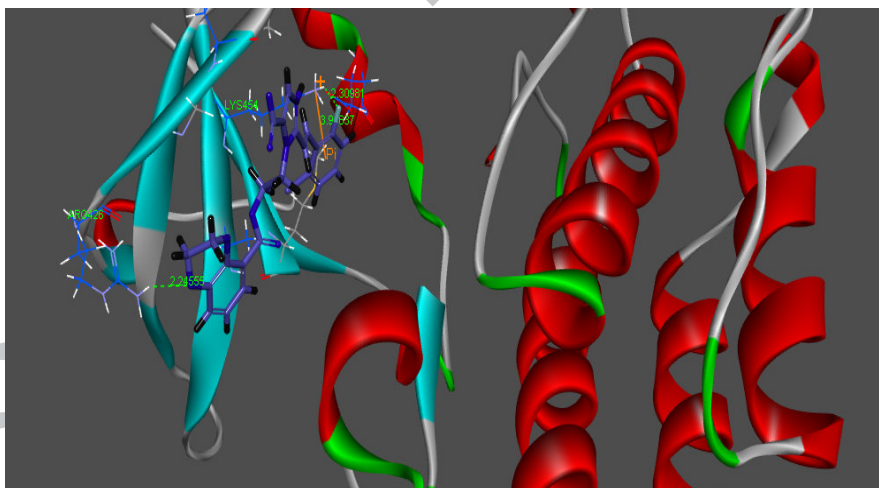
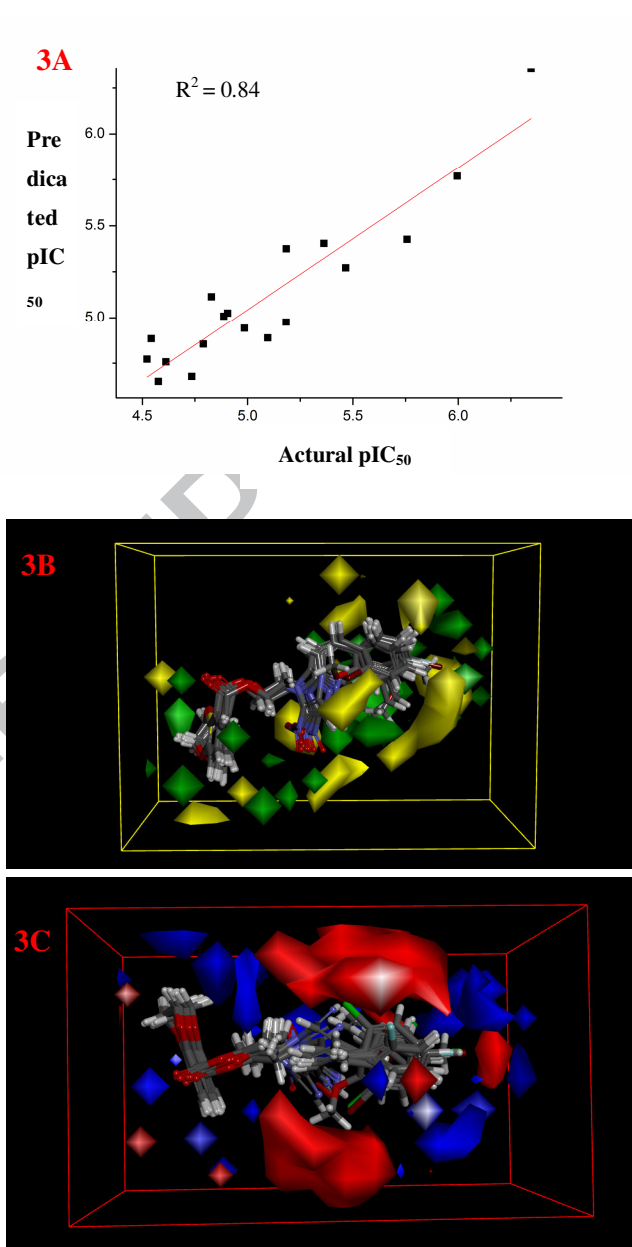
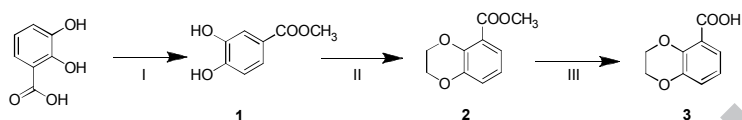


Figure 3.(3A) Using linear fitting curve to compare the predicted pIC₅₀ value with that of experiment.(3B) Isosurface of the 3D-QSAR model coefficients on electrostatic potential grids. The blue triangle mesh represents positive electrostatic potential and the red area represents negative electrostatic potential. (3C) Isosurface of the 3D-QSAR model coefficients on Van der Waals grids. The green triangle mesh representation indicates positive coefficients; the yellow triangle mesh indicates negative coefficients.

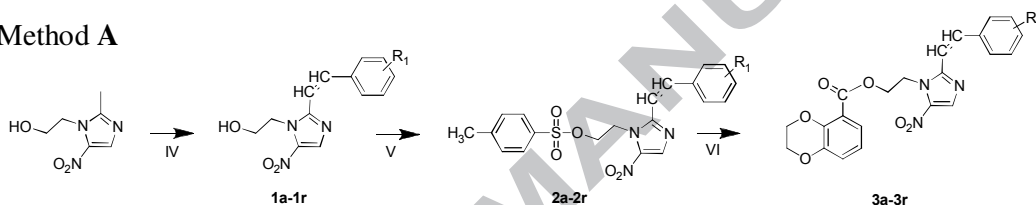


Scheme 1.General method of the preparation of compounds **3a-3r**. Reagents and

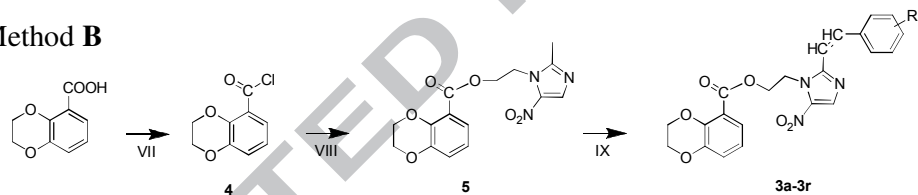
conditions: (I) methanol, concentrated sulfuric acid, 90 °C, 8 h; (II) dibromoethane, potassium carbonate, acetone, 70 °C, 12 h; (III) NaOH (aq), MeOH, THF (85–95%); Method **A**: (IV) Sodium methoxide, different aldehydes, DMSO, methanol, room temperature, 4h; (V) 4-toluene sulfonyl chloride; CH₂Cl₂, TEA, room temperature, 5 h. (VI) 2,3-dihydro-1,4-benzodioxine-5-carboxylic acid, DMF, K₂CO₃, reflux, overnight; Method **B**: (VII) SOCl₂, DMF, reflux, 4 h; (VIII) CH₂Cl₂, TEA, 8 h. (IX) NaOH, different aldehydes, DMSO, methanol, room temperature, overnight.



Method A



Method B



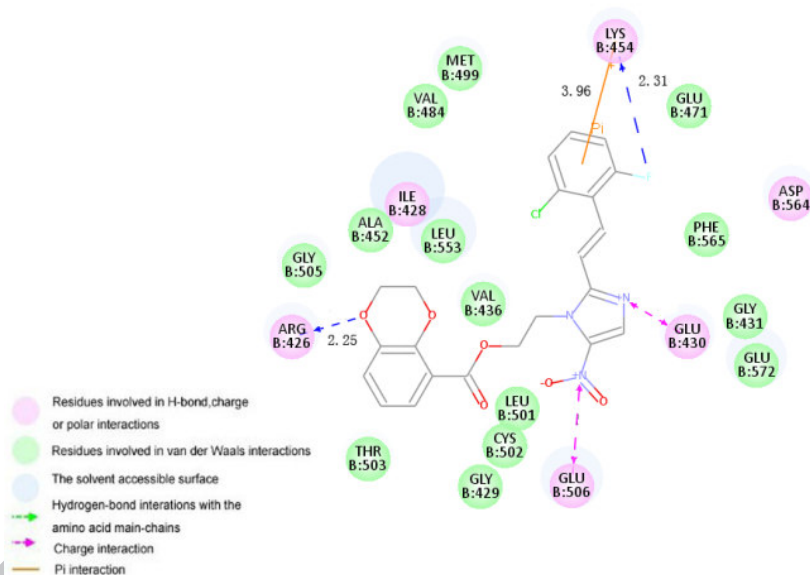
R= **3a**: *o*-Cl; **3b**: *m*-Cl; **3c**: *p*-Cl; **3d**: *o*-Br; **3e**: *m*-Br; **3f**: *p*-Br; **3g**: *o*-F; **3h**: *m*-F; **3i**: *p*-F; **3j**: *o*-CH₃;

3k: *m*-CH₃; **3l**: *p*-CH₃; **3m**: *o*-OCH₃; **3n**: *m*-OCH₃; **3o**: *p*-OCH₃; **3p**: 2-F-6-Cl; **3q**: fused Ph; **3r**: H

**Synthesis, biological evaluation, and molecular docking studies of
novel 2-styryl-5-nitroimidazole derivatives containing
1,4-benzodioxan moiety as FAK inhibitors with anticancer activity**

Yong-Tao Duan[†], Yong-Fang Yao[†], Shashikant B. Teraiya, Nilesh j. Thumar,
Dan-Jie Tang, Xiang-Xiang Tao, Ai-Qin Jiang*, Hai-Liang Zhu*

State Key Laboratory of Pharmaceutical Biotechnology, Nanjing University, Nanjing 210093,
People's Republic of China



A series of 2-styryl-5-nitroimidazole derivatives containing 1,4-benzodioxan moiety (**3a-3r**) has been designed, synthesized and their biological activities were also evaluated as potential antiproliferation and focal adhesion kinase (FAK) inhibitors. Among all the compounds, **3p** showed the most potent activity *in vitro* which inhibited the growth of A549 with IC_{50} value of $3.11 \mu M$ and Hela with IC_{50} value of $2.54 \mu M$ respectively. Compound **3p** also exhibited significant FAK inhibitory activity ($IC_{50} = 0.45 \mu M$). Docking simulation was performed for compound **3p** into the FAK structure active site to determine the probable binding model.